

PERFORMANCE OF SOME DIFFERENT FGGE OBSERVATION SUBSETS FOR A PERIOD IN NOVEMBER 1979

Per Kållberg

Swedish Meteorological and Hydrological Institute
Norrköping, Sweden 1)

1. INTRODUCTION

One major objective of the FGGE was to evaluate and compare the performance of different types of new observing systems, in particular their impact on global analyses and numerical forecasts. During the FGGE year a global observational dataset ('level II-b dataset') with a coverage and quality not achieved before, or after, was assembled (Bengtsson et al., 1982). These data have been used for several observation impact studies, reported at the present seminar, and elsewhere. In this study we will concentrate on automated aircraft data (ASDAR/AIDS) and satellite temperature profile data (SATEM) during a period in November 1979.

When examining the behaviour of an observing system in an objective analysis/numerical forecast scheme, two lines of approach are common, Observing System Experiments (OSE) and Observing System Simulation Experiments (OSSE). In the former approach, real observations, with their actual geographical distribution and actual errors, are used, while in the latter 'observations and observation errors' are generated in a controlled manner from a consistent meteorological field, usually a numerical forecast. In both approaches parallel data assimilations, including and excluding the particular observation subset to be studied, are performed. Evaluation usually consists of comparison of analyses with observations, analyses with analyses, forecasts with verifying analyses and forecasts with forecasts. Furthermore, the experiments can be classified as 'single system' experiments where a single additional observing system ('experiment') is compared with a 'minimum' ('control') analysis, for instance using only conventional, ground based observations (TEMP, PILOT, SYNOP, SHIP), or 'best mix experiments', where several systems are tested together in different combinations.

Due to imperfections both in data distribution and in data quality, there are great difficulties to extract clear signals of data impact from ensemble OSEs; the impact of a particular observation set is easily swamped by other, irrelevant factors such as sparsity of control observations or forecast errors. In OSSEs, on the other hand, ideal experimental conditions can be generated, which makes the data impact much easier to identify.

1) Present affiliation. This work was done at ECMWF.

Thus OSSEs have a tendency to overemphasize the impact of a particular observational system, while it may be underestimated in an imperfect OSE. When using real data in OSEs a general feature of the evaluations, at least from our experience at ECMWF, is the great variability of the impact from one analysis to the next, and from one geographical location to another. Such variations cannot always be anticipated, if, for instance, the first guess forecast happens to be good for a certain synoptic system, the presence or absence of data may not be crucial for the forecast development of that particular system. On the other hand, it may happen that even a single observation is absolutely essential to get a reasonably realistic analysis of another system that is not present in the first guess forecast.

A consequence of this is that many cases are needed to detect any systematic impact in the statistical average; too small samples give unreliable results which may be modified if more cases are added to the ensemble. With the effort needed, both in computer time and manpower, exhaustive statistical evaluations of OSEs are still almost impossible, at least if several observation subsets are to be tested. On the other hand, in individual synoptic situations the data impact may be very easily demonstratable, as already pointed out. Thus case studies have to be an important part of OSE evaluations.

Another difficulty in examining the impact of different analyses on numerical forecasts has been described by Arpe et al. (1985). In a set of experiments where three different analysis/forecast systems were intercompared, using the same FGGE input data, it was clearly demonstrated that in the time range 2 to 6 days, i e the range of prime interest for medium range forecasting, the total prediction error was dominated by the inherent errors of the forecast models. The analysis errors, or differences, dominated the total error only during the first day. A consequence of this finding is that even rather clear analysis differences due to the presence-absence of a certain observation set are quickly hidden by forecast errors. Neither the experiment, nor the control forecast may verify very well against analyses. Thus evaluation of OSE forecasts by comparison with verifying analyses is very difficult. Fortunately, the impact of analysis differences on the ensuing forecasts is easier to identify by comparing forecast against forecast. Since the same forecast model is used for control and experiment, the temporal increase of the amount of separation between the two forecasts is due only to analysis differences, i e the impact of the observations.

Based on those experiences and reasonings, the data impact study reported here concentrates on one hand on a particular case study (section 3), and on the other on average forecast separation (section 4). In section 2 the setup of the experiment is described and in section 5 some conclusions are drawn.

2. THE EXPERIMENT

In the present paper, an OSE, using FGGE data from November 1979, is described. The main aim was to look into the impact of satellite temperature profiles (SATEM) and automated aircraft observations (AIDS/ASDAR). Based primarily on data availability, two polar orbiting satellites were available from the middle of October, but also on synoptic activities, a period from November 8 to 18 was selected. For this period eight parallel data assimilations were performed, using the version of the ECMWF data assimilation system available at the time of the experiments. This version differs from that used for the ECMWF level III-b analyses (Bengtsson et al., 1982) in several aspects, the most important being the vertical interpolation between analysis pressure levels and initialization-forecast σ -levels. In the present assimilations the so-called incremental interpolation was used. A modified, somewhat steeper orography was also used.

A subset of the assimilations was used for a comprehensive OSE on aircraft data (Baede et al., 1985) where more details on the experiment setup can be found. The eight different experiments are summarized in Table 1, where the acronyms used for each assimilation are defined. These acronyms, although sometimes illogical, will be used throughout this paper to identify the experiments.

Experiment acronym	Ground-based*	Buoys	Aircraft	SATOB	SATEM
AI	YES	YES	YES	YES	YES
AO	YES	YES	NO	YES	YES
SO	YES	YES	NO	NO	NO
SX	YES	YES	YES	NO	NO
SB	YES	YES	NO	YES	NO
SM	YES	YES	NO	NO	YES
N1	YES	YES	NO	NO	ONE ONLY
SP	NO**	YES	YES	YES	YES

* TEMP/PILOT/SYNOP/SHIP

** Surface pressure data used

Table 1 Summary of assimilation characteristics

The total set of FGGE level II-b data (we used the so-called 'main II-b' dataset) was divided into five categories, ground based (= TEMP, PILOT, SYNOP, SHIP), buoys (= DRIBU), aircraft (= AIREP, AIDS, ASDAR), satob (SATOB, = cloud drift winds) and satem (SATEM = IR and μ -wave soundings from satellites).

There are two control experiments, one using all data (AI) and one using only ground based data (SO). The other experiments contain different subsets of AI. In experiment SP the ground based data were removed in order to simulate a possible completely automated space-based observing system. To simulate automated pressure sensors on land and drifting buoys, surface pressure data were, however, retained in experiment SP. The FGGE drifting buoys were used in all assimilations, so far we have not made any OSE specifically addressing the buoy data.

A typical example of data distribution during the experiment is shown in Figure 1. From the maps the obvious fact that aircraft data are primarily available from the main air routes of the world is clearly seen. Although the November period was selected partly because two polar orbiting satellites were operational, the SATEM map only shows one satellite. This was actually not too unusual during the period, large gaps now and then occurred in one or the other of the TIROS-N and NOAA-7 satellite coverages. In particular, the area immediately west of North America frequently showed gaps due to operational practises. The DRIBU coverage was very good during the period.

From each of the eight assimilations, seven forecasts were run, using the same version of the (then) ECMWF gridpoint model as was used in the assimilations. The forecast cases are listed in Table 2. Forecast verifications were carried out against the ECMWF level III-b analyses. Large amounts of maps showing analyses, forecasts, forecast minus analysis and forecast minus forecast were produced as well as other diagnostics.

Forecast number	Initial data
1	10 Nov 00GMT
2	11 Nov 00GMT
3	13 Nov 00GMT
4	16 Nov 00GMT
5	18 Nov 12GMT
6	14 Nov 12GMT
7	11 Nov 12GMT

Table 2 Initial times of the seven forecasts. For each time all eight cases were run up to +10 days.

3. A CASE STUDY

In this section we will focus on one particular situation on the North Pacific Ocean from November 11th 00GMT. This case was found to be one of the better examples of a synoptic development where the impact of different data types could be demonstrated. The data coverage at the time of analysis is seen in Figure 1. Figures 2 and 3 show the 250mb and surface analyses from the complete (AI) dataset, including available observations. The central area is characterized by very few upper air stations, only the Aleutians, Midway Island and, to the east, ship PAPA, and thus the upper air analyses are primarily defined by aircraft wind data, centered around 250mb and SATEM thickness data available throughout the atmosphere. There are also a limited number of SATOB data, centered around the cirrus level and around 900mb. At the surface a reasonable amount of SHIP data are available.

The feature of prime interest is the upper level trough at 30 N, 170 E, with an incident weak surface low at 20 N, 170 E. In 48 hours the surface low has developed into an intense cyclone with surface easterlies of more than 30 m sec⁻¹ at 33 N, 175 W, see the AI analysis from 00GMT, November 13th in Figure 4. The 250mb trough has developed into a cut-off cyclone centered at 29 N, 179 E.

The minimum, ground based observing system (SO) is almost void of upper air data, and the initial analyses are very different (Figure 5), from AI at 250mb. A map of the difference between the two analyses shows height differences up to 182 gpm and vector wind differences up to 44 m sec⁻¹ (Figure 6). At the surface the analyses are much more similar with pressure differences never exceeding 3mb anywhere in the area.

The very marked impact on the 250mb analyses is due to the combined effect of SATEM, SATOB and aircraft data. To try to separate what role each observing system plays, the 250mb difference maps 'AO-SO' (Figure 7) 'SX-SO' (Figure 8) 'SM-SO' (Figure 9) and 'SB-SO' (Figure 10) are displayed. It can first be noted that AO-SO and SM-SO are very similar, indicating that the SATOB data added in AO hardly add any information.

On the other hand, SB-SO also shows the same main trough-ridge pattern, although with some differences. Obviously the SATOB data, at Nov 11 00GMT and earlier contain useful data per se, which help to improve the SB analysis compared to SO. There is some amount of redundancy in the SATOB data.

The differences AO-SO (or SM-SO) are due to the SATEM thickness data. The height patterns have a large scale with a positive discrepancy at 35°N, 180°E and a negative at 45°N, 165°W. Bi-modal height difference patterns of this type indicate a phase difference between the two components.

The SATEM thickness data contribute to improve the analyzed position of the large scale main trough in Figure 2. Through the multivariate coupling in the data assimilation, consistent wind differences are also seen in the maps.

Now turning to the aircraft impact, a comparison of AI-SO with SX-SO indicates that the aircraft data alone are also able to improve the 250mb analysis considerably. The bimodal pattern indicating a phase error in the main trough in assimilation SO, is found in both maps. There is, however, additional impact in the structure of the developing part of trough around 30°N , 175°W . With aircraft data included, vector wind differences to SO of more than 40 m sec^{-1} occur, in the case of no SATEM (SX-SO) even 51 m sec^{-1} . The aircraft observations intensify the jet and sharpen the trough.

A crucial question when analysing single level wind data, is how their impact is distributed vertically. This problem has been discussed by, among others, Sumi (1982). In Baede et al. (1985), the present experiment is discussed in some detail from this point of view. In the ECMWF optimum interpolation a fairly wide vertical correlation was assumed for the wind first guess prediction error, which has the effect of distributing the observed wind deviation throughout a large position of the atmosphere, see Figure 11. By this assumption it is hoped that the wind data will impact the so-called 'slow manifold' (Leith, 1980) and will survive the ensuing initialization to contribute to the forecast. A comparison between our approach and the converse approach of inserting the wind data at the level of observation only, has been made by Lorenc (1982). His findings confirm that more of the aircraft wind information is projected on to the main flow in the ECMWF system. In the UKMO data assimilation system used by Lorenc, a considerable part of the aircraft information rapidly radiates away as gravity waves.

At the same time it must be pointed out that the ECMWF systems assumes that the first guess prediction error is separable into a horizontal and a vertical part. A consequence of this assumption is that only a 'barotropic' part of the aircraft wind information impacts the analysis. The full potential of the single level wind data may not yet be exploited.

The final analysis difference map, Figure 12, shows the 'space-based' system SP-SO. Even here the pattern is quite similar to that of the control, AI-SO. The space-based analysis and that from the complete FGGE dataset are mutually more similar over the North Pacific than any of them is to the ground based analysis SO. This may indicate that it is more important to have reasonably good data with a complete global coverage than high quality radiosonde data with very uneven distribution between land and ocean. A reservation to this statement is, however, that the AI control analysis to a large extent is defined by space based systems over the ocean, highlighting the inherent difficulty of the OSE approach.

To demonstrate the importance of the analysis differences discussed above, a series of forecast difference maps AI-SO are shown in Figures 13 a-c with the initial difference of Figure 6. Over land areas, well covered by radiosonde data in SO, the forecasts are remarkably similar. The central Pacific difference on the other hand rapidly develops into the very dramatic +48h differences in 13 c, with height differences at 250mb amounting to 470 gpm and vector wind differences up to 76 m sec^{-1} .

The initial analysis difference rapidly progresses downstream with the group velocity in the manner demonstrated by, for instance, Cats and Åkesson at ECMWF (1983). It is interesting to note that, although the initial analysis differences at the surface were small, the upper air differences rapidly organize themselves into a baroclinically developing system throughout the entire atmosphere, already after 12 hours (13 a) there are pressure differences of 8mb and vector wind differences of 19 m sec^{-1} .

The +48h forecast from analysis AI (Figure 14) verifies well with the AI analysis from Nov 13 00z in Figure 4. The forecast surface low is not quite deep enough, 1004mb compared to 1001mb and its position is a bit too far west. At 250mb a cutoff low is formed, again somewhat too slow, but the overall pattern indicates a very good forecast.

The landbased, 'minimum' observing system, SO, is not able to give a useful +48h forecast for the North Pacific ocean, Figure 15. The surface low is found at 37°N , 165°W , far away from the verification, and the 250mb flow is very different, with one elongated trough stretching from Alaska towards 20°N , 175°E , instead of the double structure with a cutoff cyclone at 175°E and a deep trough at 155°W . In short, AI gives the best forecast, as expected, and SO the worst, also expected.

An examination of the other forecast cases; AO in Figure 16, SX in Figure 17, SM in Figure 18 and SP in Figure 19, gives an interesting insight into the strengths and weaknesses of the aircraft and SATEM observations respectively. Beginning with AO, we see that the development is less intense, both at the surface and at 250mb, while the position of disturbances are similar to those in AI. The single level wind data have assisted in sharpening initial gradients in order to give the observed intense development. In AO some single level wind data were still used, i.e. those from the cloud drift winds, SATOB. When they are removed too, in experiment SM, hardly anything remains of the surface development, Figure 18. The large scale 250mb features are still in their correct positions, although the cut-off low now is very weak.

The SX forecast in Figure 16, shows a very intense development at the surface, similar to that in the complete AI case. The central pressure of the cyclone is 1005mb. It is hard to give a definite judgement on which is the better, possibly it can be said that a line connecting the anticyclonic center to the north with the cyclonic center, which in the verification runs straight from north to south, is somewhat better predicted in AI than in SX.

Finally, the space-based forecast, SP in Figure 19, also gives the main features of the development in a reasonable way. The surface low is too weak, and too slow, and the 250mb cut-off low too far to the southwest. Still the SP forecast is clearly better than that from the groundbased system in experiment SO.

Concluding this subjective evaluation of one single case, it can be stated that the complete FGGE level II-b dataset gives the best forecast and the minimum ground based system the worst. The SATEM data are able to define the major trough-ridge pattern in a good way, but finer details, such as sharp gradients leading to baroclinic developments, are not caught. Adding single level wind data improve these features, if the data are available in the crucial positions. It is a common experience that new frontal developments in the lower troposphere are often triggered off by divergent wave disturbances at the jet stream level. A good, high resolution analysis of such disturbances may be important. In the FGGE database, the aircraft (and SATOB) single level wind data were contributing to achieve this.

The SATEM temperature profiles have a resolution of about 250 km in the level II-b database. This resolution is apparently not sufficient in defining such finer details in the initial states that may turn out to be important for successful predictions. On the other hand the SATEM data, already in the FGGE resolution, are invaluable in defining the large scale flow.

4. ENSEMBLE FORECAST IMPACT

In evaluation of OSE forecasts, a major difficulty is how to verify. The verifying analyses must, necessarily, suffer from the same problems of incomplete and erroneous data as the experimental analyses. Furthermore the inherent errors of the forecast model tend to hide the sometimes subtle analysis differences, at least after one or two days, as already discussed. One way of circumventing these difficulties is to use a control forecast as verification. The scores will then not show how good a forecast is, just how different, or separated, it is from the control. In this section we will discuss the forecast separation and how it varies in the different experiments and in different areas. The forecast separation is expressed simply as root mean square difference, gridpoint by gridpoint between the experiment geopotential height and that of the control, AI, for every 12th hour from initial state to +10 days. Other scores were also calculated, but for the purpose of discussing forecast separation in this section, only the RMS will be used. The calculations were done for 250, 500 and 850 mb. In Figures 20 a, b, c and d the separation of 250 mb geopotential is shown for both hemispheres (as defined in the caption).

In the Southern Hemisphere removal of aircraft in AO has very little impact, as expected from the data distribution, after six days the separation is not more than 20 gpm. The satellite data are, on the other hand, of paramount importance here, removing them in SO gives an initial separation of 60 gpm, which grows to 120 gpm in six days. Adding the aircraft, in SX, hardly makes any difference. Thus it can be safely stated that the southern hemisphere AI analyses are to a very large extent defined by the satellite data. Remember that the drifting buoy data were used in all our experiments, their importance for the assimilation of SATEM-data has not been studied yet by us.

In the present experiment the cloud drift winds were assigned relatively large observation errors, based on earlier experience with SATOB data from the main level II-b set at ECMWF (Källberg et al., 1982). In particular the height assignments of clouds were unreliable, or even absent, and systematic underestimating of windspeeds were also found. Thus the SATOB data were given low weights in the November assimilations, and as seen from Figure 20c, the SATEM data provide the major satellite impact on the AI analyses.

The initial separation of the SATOB analyses, SB to the control AI, is large, more than 45 gpm. Since wind data give information on mass-field gradients only, the thermal structure of the SB analyses are defined mainly by the few radiosondes and the forecast model itself. For the southern hemisphere this is not enough, it seems necessary to have a reasonably even distribution of mass data, which can only be achieved by the SATEM profiles.

The initial separation SB to AI does not grow appreciably during the first day of the forecast, either in the southern (Figure 20c) or the northern (Figure 20d) hemisphere. Such a behaviour would not be unreasonable if the SATOB data are assumed to contain information that is not representative of the large scale flow, as it is observed in AI. Local, small scale wind systems, given by the cloud drift data, may degenerate rapidly and not have a major impact on the medium range forecasts.

In Figure 20c we also note that the space-based system, SP, is the second closest to AI, next to SM only. Again this shows that the control analyses AI are, to a very large extent, defined by the satellite profiles.

In the northern hemisphere (20°N - 82.5°N) the aircraft data availability, and impact are very different, Figures 20b and 20d. As on the southern hemisphere, the AO forecasts are closest to AI, but the separation is larger, almost 60 gpm at +6 days, compared to 20 in the south.

The ground-based data alone, in SO, give a very different development with a +6 day separation of 110 gpm. This is almost as much as in the southern hemisphere, albeit the initial separation is much less, only 25 gpm compared to 60 gpm in the south. High resolution, high quality radiosonde data over inhabited continents are not sufficient to define the hemispheric flow with an accuracy sufficient for medium range forecasts.

Of the three single system experiments: SX for aircraft, SM for SATEM and SB for SATOB, SX and SM give very similar separations to AI of about 15 gpm initially and 65 to 70 gpm at day 6. SB is further off, 19 gpm initially and about 90 gpm at day 6. The space-based system, SP, shows about the same separation to AI as the ground-based, SO.

Just as the case study in the previous section, the ensemble separation statistics indicate that the aircraft wind data contain much valuable information, which the assimilation system is able to exploit to an appreciable extent. The result that the SX and SM separations are of the same order indicates that both systems contribute to the definition of the full FGGE analyses; the single level aircraft winds are a very good complement to the SATEM profiles. This is also underlined by the combination SM+SB, in experiment AO, which shows the smallest separation. Even if SB itself is quite far from the control, addition of the SATOB single level winds is beneficial to the analyses in AO.

5. CONCLUSIONS

Of all the different diagnostics that have been studied in the evaluation of the November OSE, we have concentrated on only two in this lecture. Nevertheless, it is possible to draw some general conclusions on the relative performance of several of the observing systems tested during the FGGE. These conclusions refer to middle and high latitudes only. The data impact in the tropics is not discussed here.

- The satellite temperature profiles are absolutely essential to define the large scale flow pattern, not only on the southern hemisphere, but also over oceans and other uninhabited parts of the northern hemisphere. The ground-based radiosonde system is not sufficient to give a good analysis of the hemispheric flow on either hemisphere.
- The resolution of the FGGE 'Main level II-b' SATEM data, about 250 km or more is too low to analyze some fine-scale synoptic structures essential for short and medium-range forecasts.
- Single level wind data are very useful to enhance the resolution of analyses over areas without good radiosonde networks. They constitute an excellent complement to coarse (250 km) resolution SATEM data.
- Aircraft observations, AIREP, ASDAR provide single level wind data of very good quality. ASDAR is better than AIREP due to higher density and the elimination of position errors.
- In the Main FGGE II-b database the SATOB cloud drift winds had lower quality than the aircraft data, primarily due to difficulties in height assignment. They still provide useful information not available in other ways, particularly in the tropics.
- The problem of how to extract the full potential use of single level wind data is not yet solved.
- An imagined future observing system, using only fully automated space-based data extracted from the FGGE database, clearly outperforms the ground-based system in the southern hemisphere. In the northern hemisphere this system is as good as the present ground-based one.

In spite of the arguments so far, comparing the relative performance of the different observing systems to each other, the final aim of any observation system evaluation is to find out how good the forecasts are. All the experimental forecasts in Table 2 have been verified against the ECMWF FGGE level III-b analyses.

These analyses were prepared from the same observations as assimilation AI, but with a somewhat older version of the data assimilation system (Bengtsson et al., 1982). In Table 3 below the average time to reach an anomaly correlation of 60%, a measure of predictability commonly used at ECMWF, is given for the 500mb geopotential height for both hemispheres and all experiments (except N1).

It should be mentioned that the correlations were calculated gridpoint by gridpoint, and not in the Fourier wavenumber space commonly used at the centre.

Experiment	Northern hemisphere	Southern hemisphere
AI	7.3	5.3
AO	7.2	5.3
SX	7.0	3.5
SO	5.7	3.5
SM	7.0	5.0
SB	6.3	5.2
SP	5.7	4.9

Table 3 Number of days to reach a 500mb height anomaly correlation of 60%. Average of seven forecasts in each experiment. Verification is done against the III-b analyses.

These scores clearly support the conclusions already given.

This experiment, although containing many assimilations and many forecasts, still cover only a short period. In order to get some insight into the danger of drawing conclusions from just one short experiment, a second set of assimilations and forecasts was run. Some results from this set are presented by Tibaldi at this seminar. Although there are some differences, the second experiment confirms the present results.

ACKNOWLEDGEMENT

The set of observation system experiments carried out at ECMWF has been a joint effort by many members of the Centre's staff and visiting scientists. Of all these people I would like to mention just one, Sakari Uppala, without whom the OSE could not have been carried through. The Centre's Director, Lennart Bengtsson, has been a continuous source of ideas, inspiration and practical assistance. Finally, I would like to thank Kerstin Fabiansen for the patient and skillful typing.

REFERENCES

- Arpe, K., A. Hollingsworth, A.C. Lorenc, M.S. Tracton, S. Uppala, P. Kållberg, 1985:**
The Response of Numerical Weather Prediction Systems to FGGE level II-b Data, Part II: Forecast Verifications and Implications for Predictability. Q.J.R. Met. Soc. No 1, 1985. (See also lecture by A. Hollingworth at this seminar).
- Baede, A.P.M., P. Kållberg and S. Uppala, 1985:**
Impact of Aircraft Wind Data on ECMWF Analyses and Forecasts during the FGGE Period, 8-19 November 1979. ECMWF Technical Report No , 1985.
- Bengtsson, L., M. Kanamitsu, P. Kållberg and S. Uppala, 1982:**
FGGE 4-dimensional Data Assimilation at ECMWF. Bull. Am. Met. Soc. Vol 63, No 1, Jan 1982.
- Cats, A.J. and O. Åkesson, 1983:**
An investigation into Marked Difference between Two Successive ECMWF Forecasts of September 1982. Contr. Atm. Phys. 56, pp 440-451.
- Kållberg, P., S. Uppala, N. Gustafsson, J. Pailleux, 1982:**
The Impact of Cloud Track Wind Data on Global Analyses and Medium Range Forecasts. ECMWF Technical Report No 34.
- Leith, C.G., 1980:**
Non-linear normal mode initialization and quasi-geostrophic theory. J. Atm. Sci. 37, pp 958-968.
- Lorenc, A.C., 1982:**
The Impact of Aircraft Data on the Meteorological Office FGGE Data Assimilation Suite: November 1979 Case Study. Met. O.20 Technical Note No II/190.
- Sumi, A., 1982:**
On an evaluation of Data Impact with respect to Rossby Mode in the Data Assimilation Cycle. Part 1, J. Met. Soc. Japan, 60, pp 917-930.

00 GMT	SUNDAY NOVEMBER 11 1979
SYNOPS, SHIPS,	2343 1076
SAT WINDS (LOW LEVEL)	674
SAT WINDS (HIGH LEVEL)	873
ASDARS, AIDS, AIREPS,	184 524 773
BUOYS, NAV AIDS, DSONDES, COLBAS	867 0 0 0
TEMPS, PILOTS,	714 466
SATEMS, LIMS SOUNDINGS	2128 0

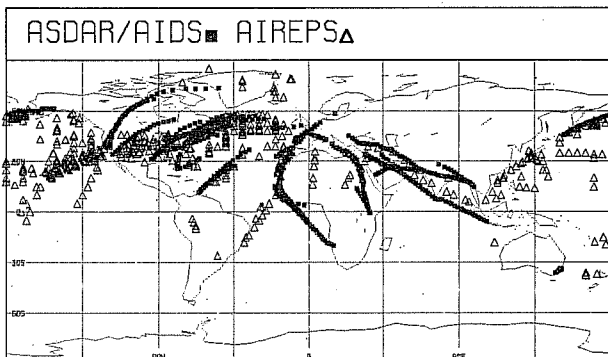
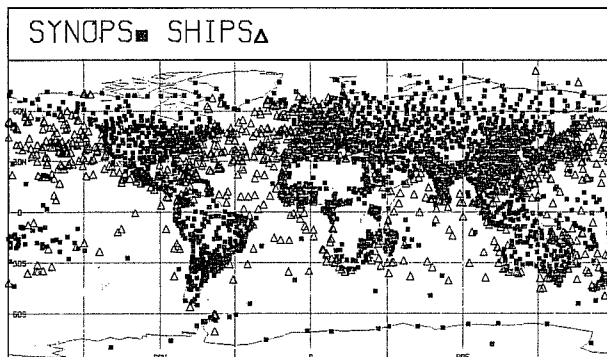
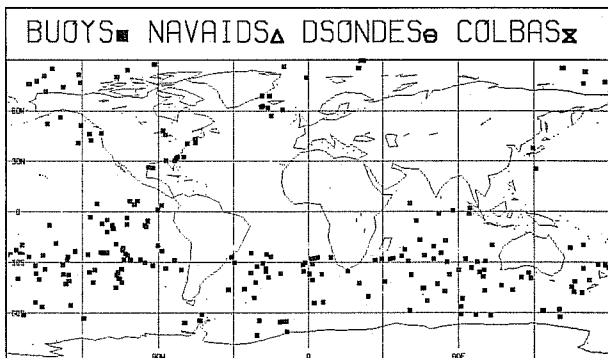
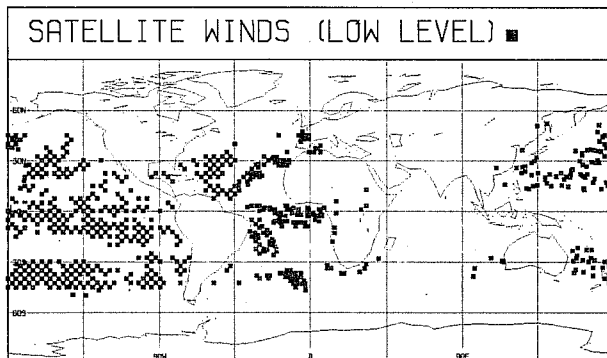
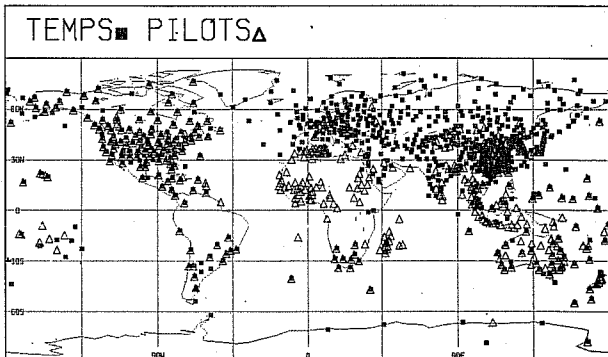
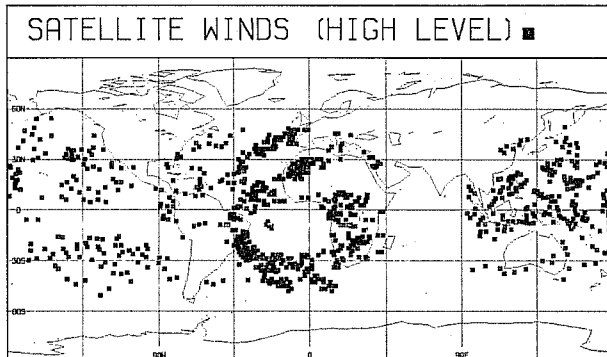
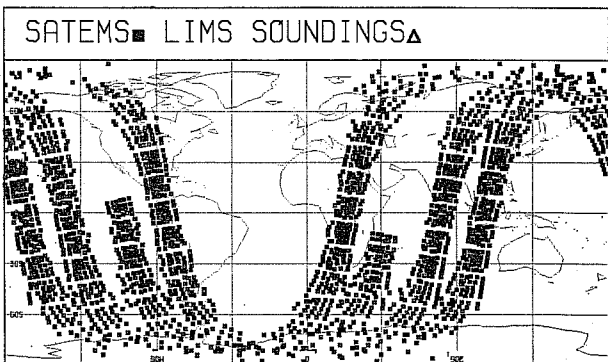


Fig. 1 Data coverage for November 11 1979 00GMT + 3 hrs.

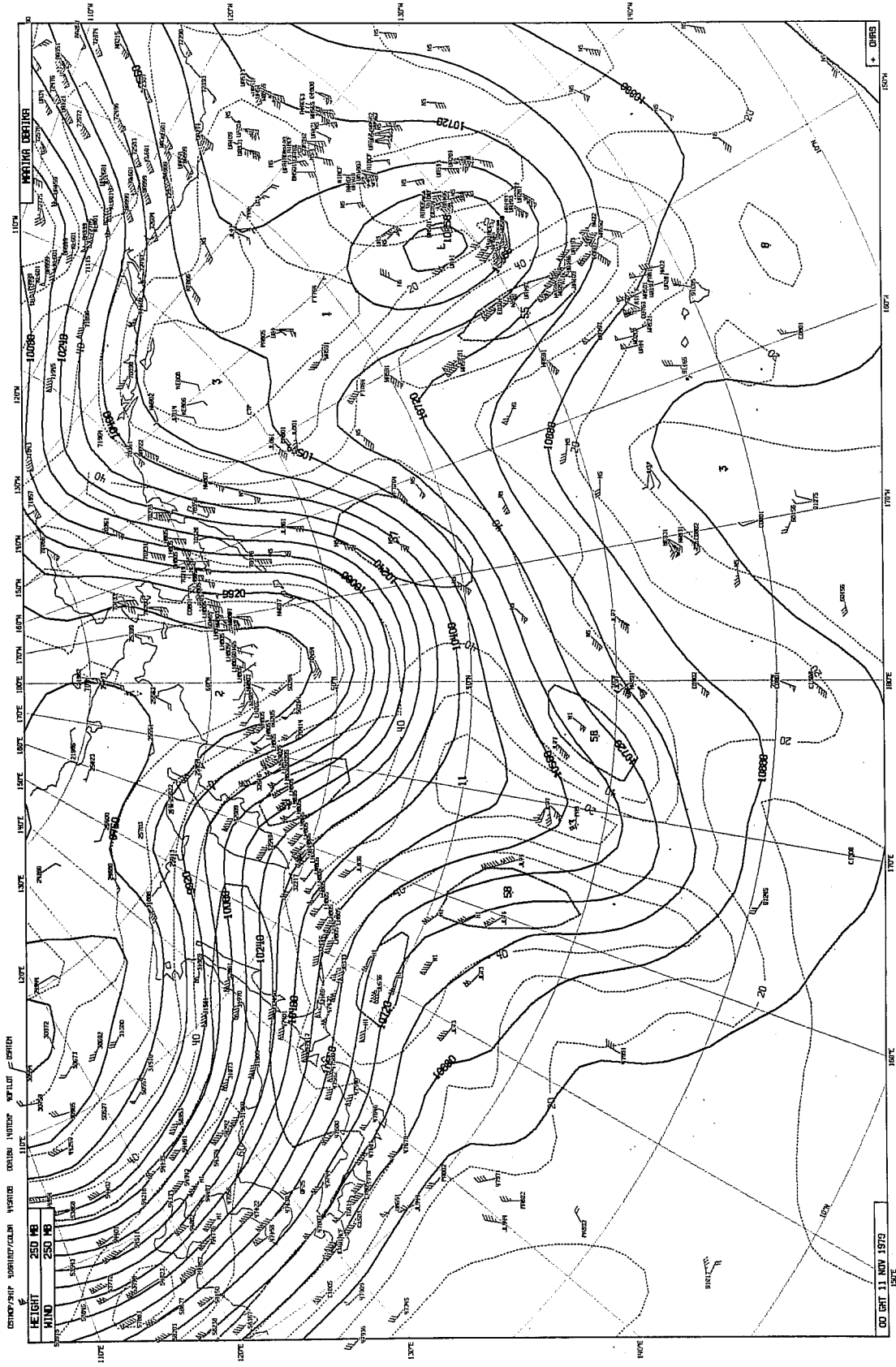


Fig. 2 250mb analysed heights (full lines) and isotachs (dashed lines) with FGGE Level II-b observations within \pm 50mb for 00 GMT, 11 November. RS winds are identified by 5 digit numbers and SATOB by 2 letter acronyms; other data are AIRCRAFT data.

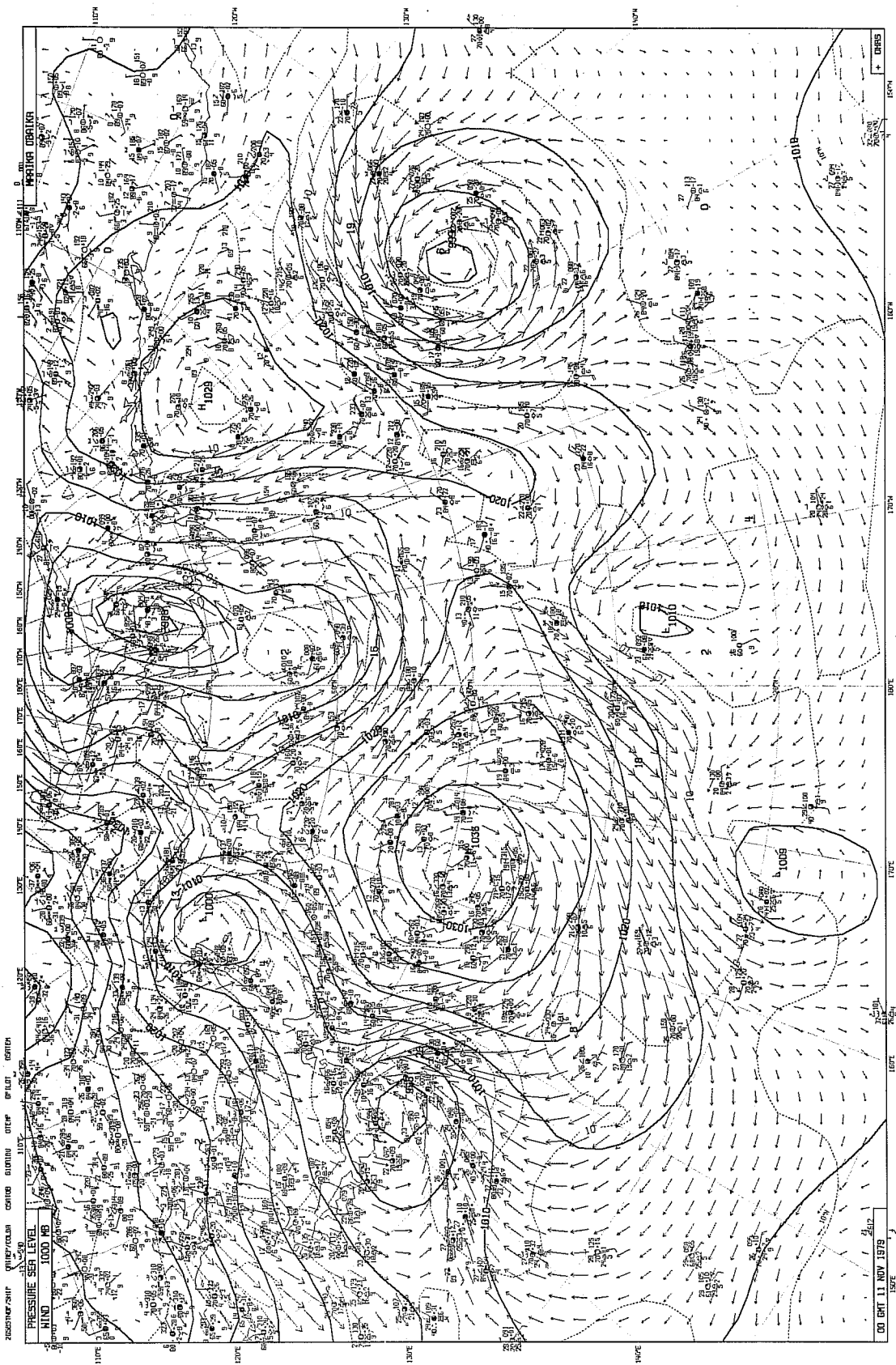


Fig. 3 Sea level pressure (full lines) and 1000mb wind analyses (arrows and isotachs) with plotted SYNOP and SHIP data for 00 GMT 11 November.

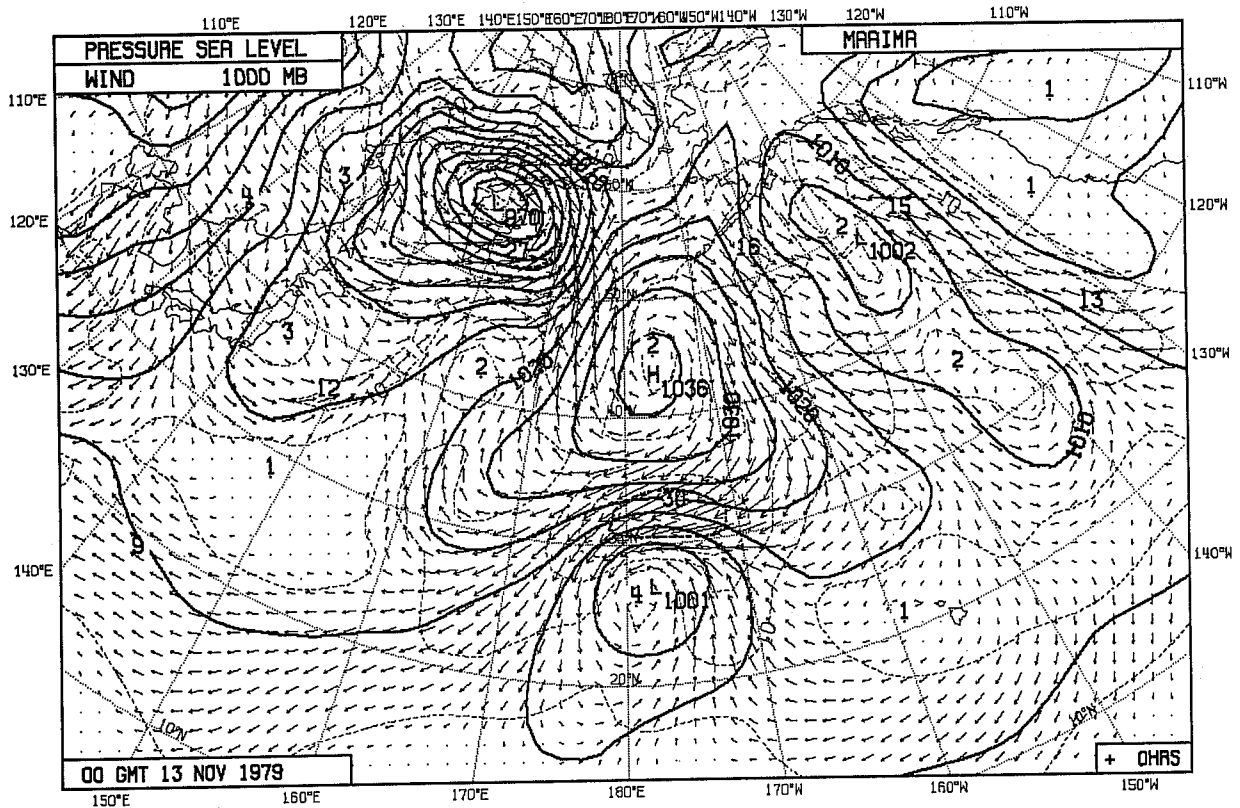
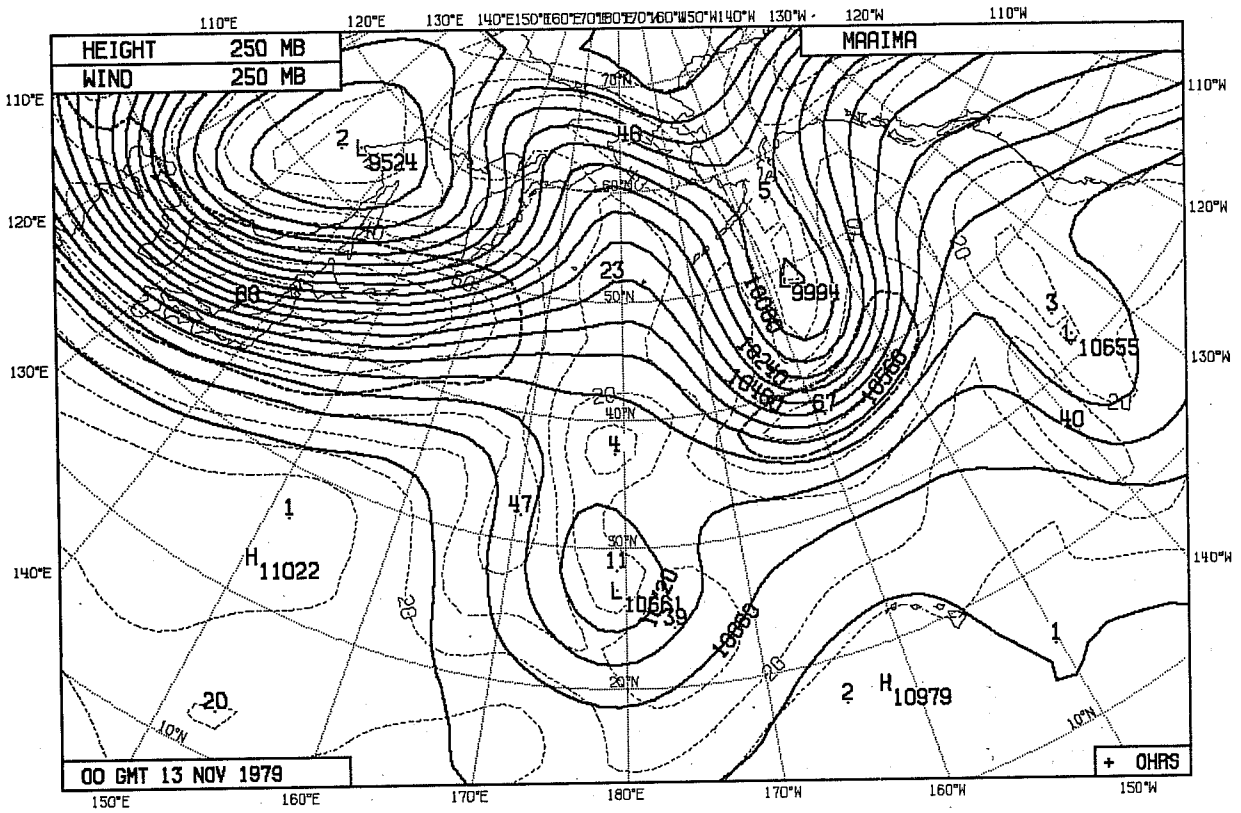


Fig. 4 250mb (top) and sea level (bottom) analyses for 00 GMT 13 November. Contours as in Figs. 2 and 3.

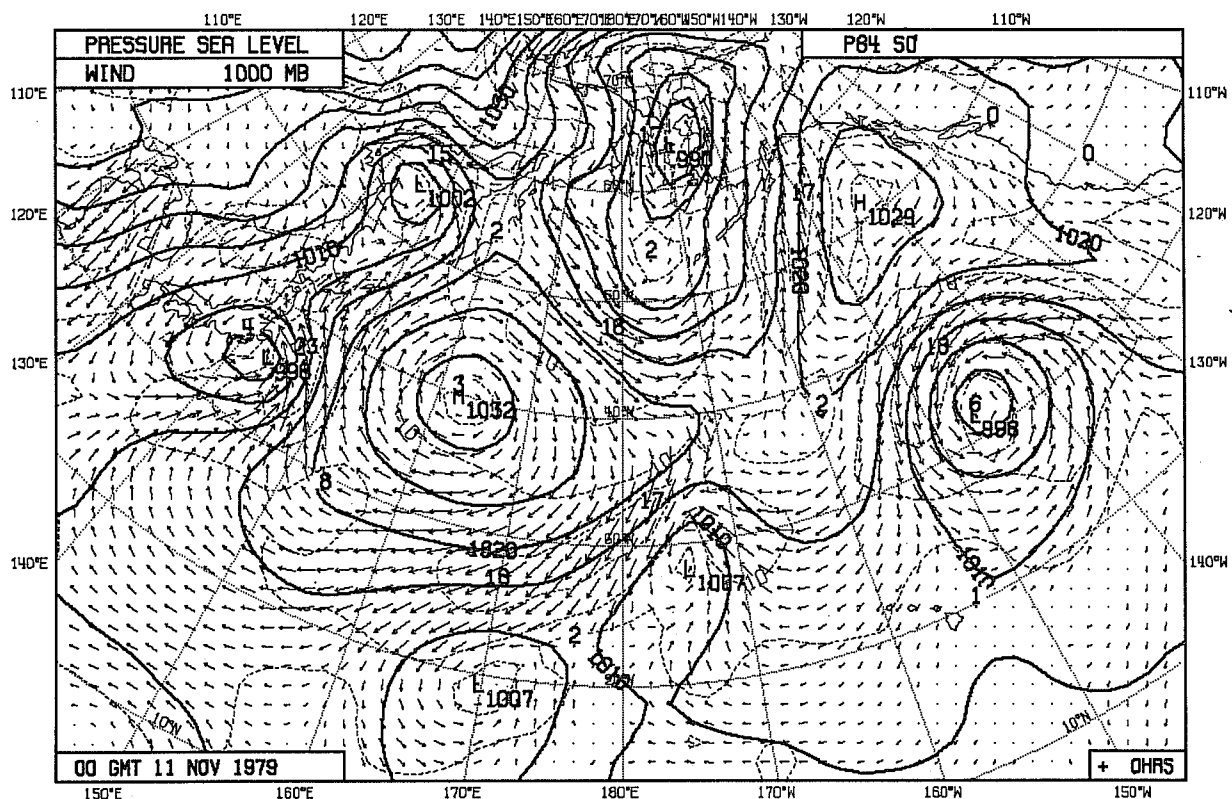
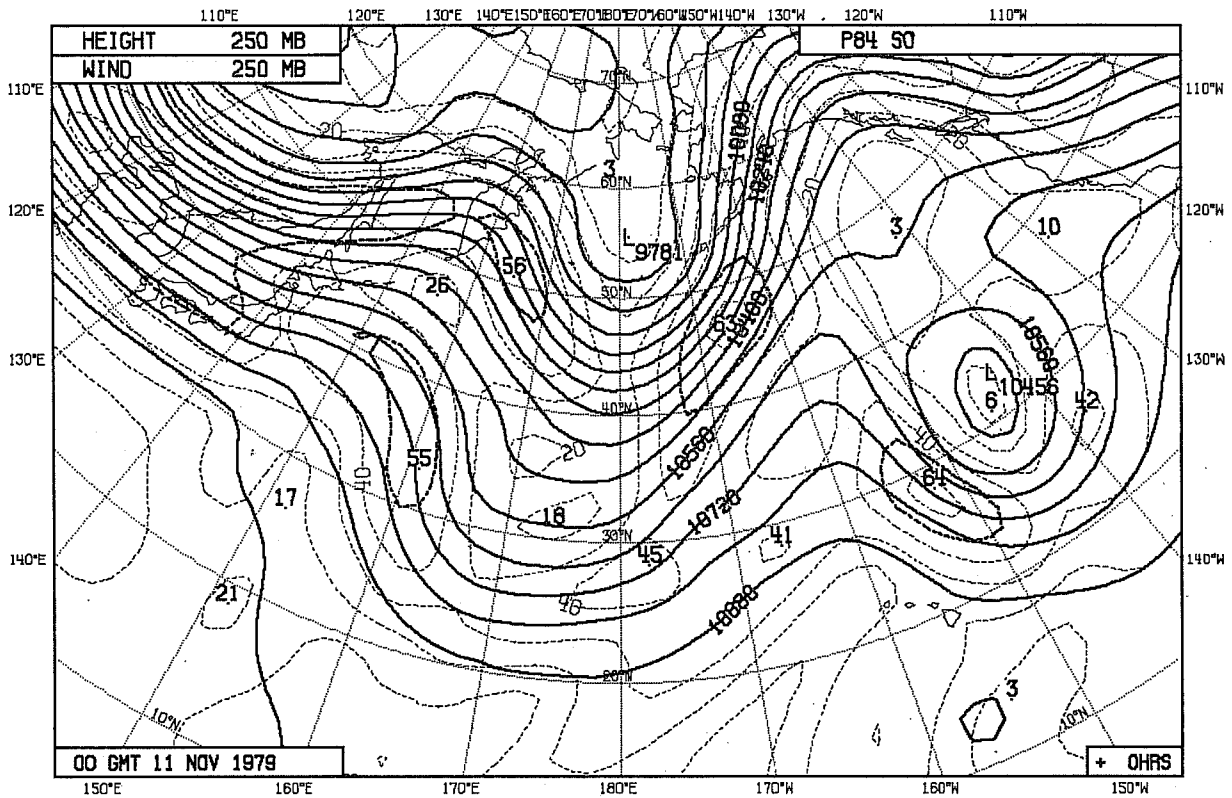


Fig. 5 250mb (top) and sea level (bottom) analyses for 00 GMT 11 November from the minimum ground bases system S0 (satellite and aircraft data excluded).

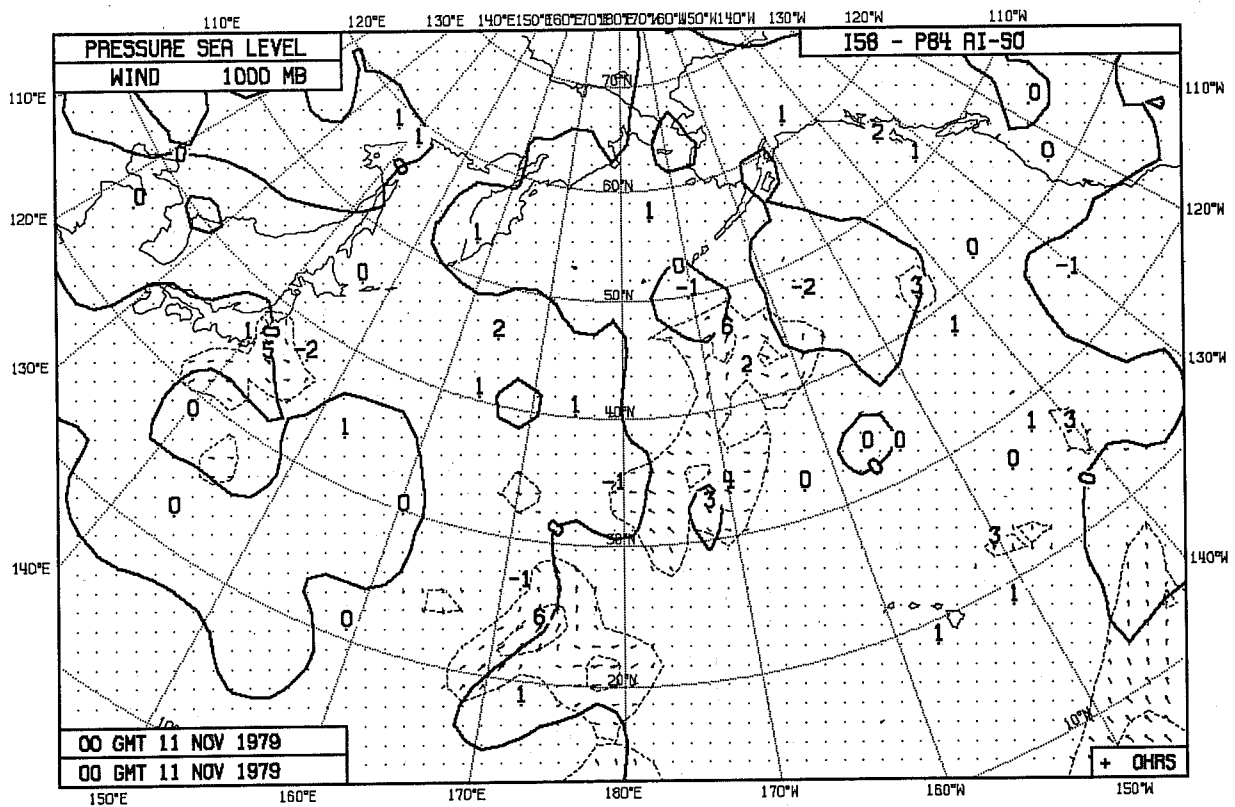
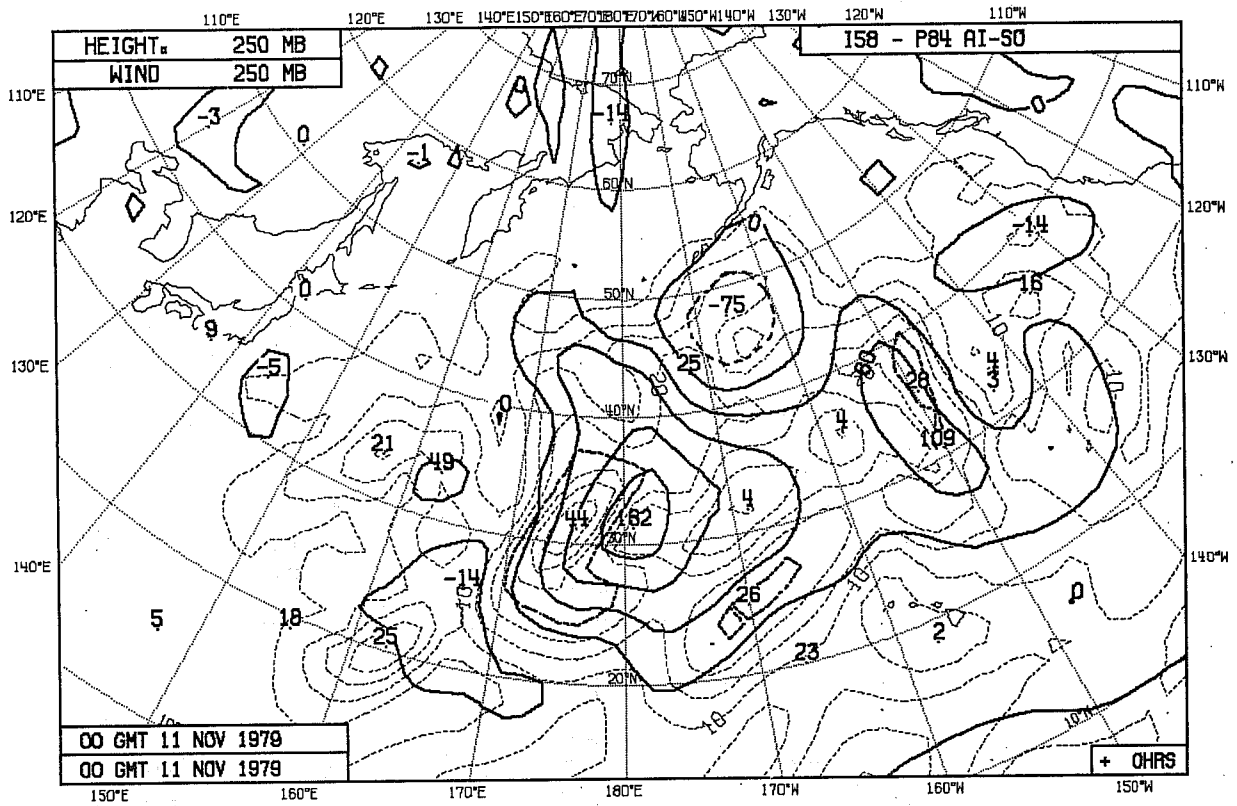


Fig. 6 Initial difference between the complete FGGE analyses (AI) and the minimum analysis (SO) for 00 GMT 11 November. 250mb heights and isotachs (top); sea level pressure and 1000mb winds (bottom).

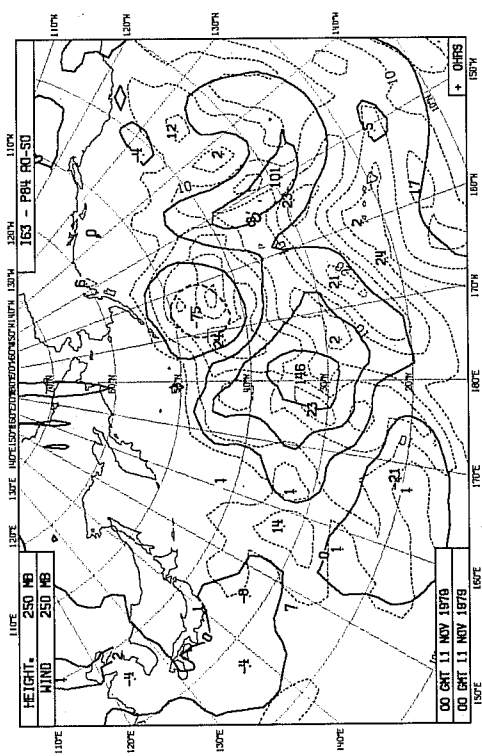


Fig. 7 250mb height and wind speed differences between the AO and SO analyses (AO-SO) for 11 November.

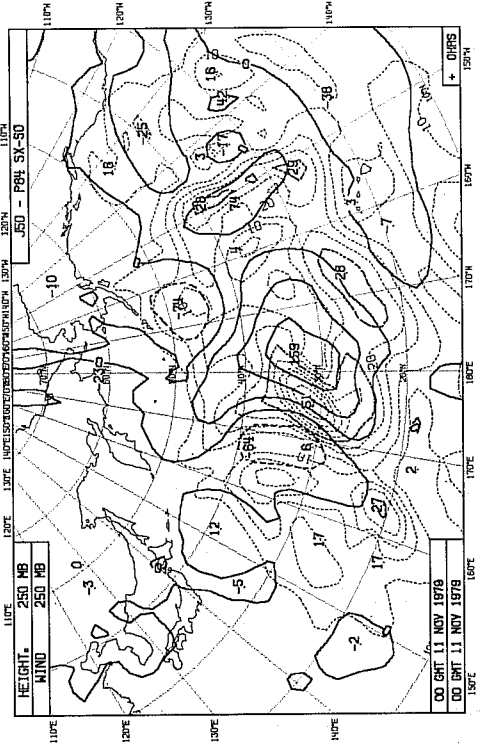


Fig. 8 As Fig. 7, but for SX-SO.

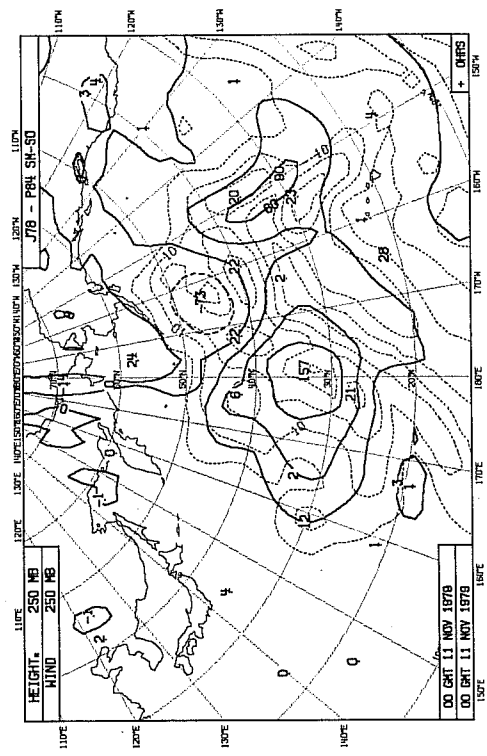


Fig. 9 As Fig. 7, but for SM-SO.

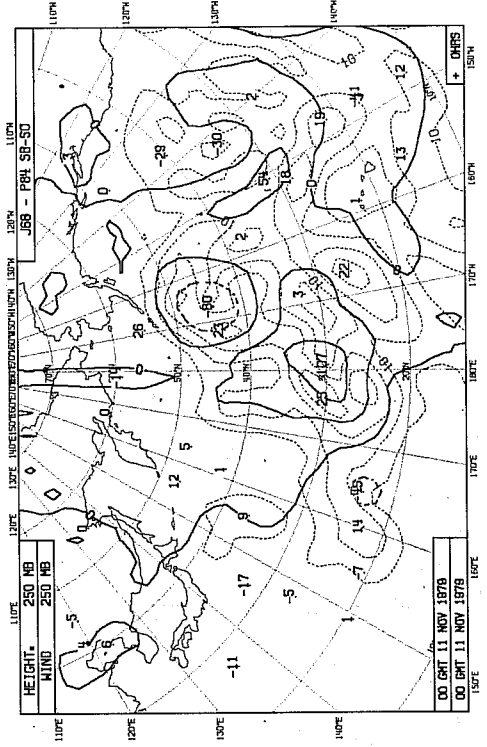


Fig. 10 As Fig. 7, but for SB-SO.

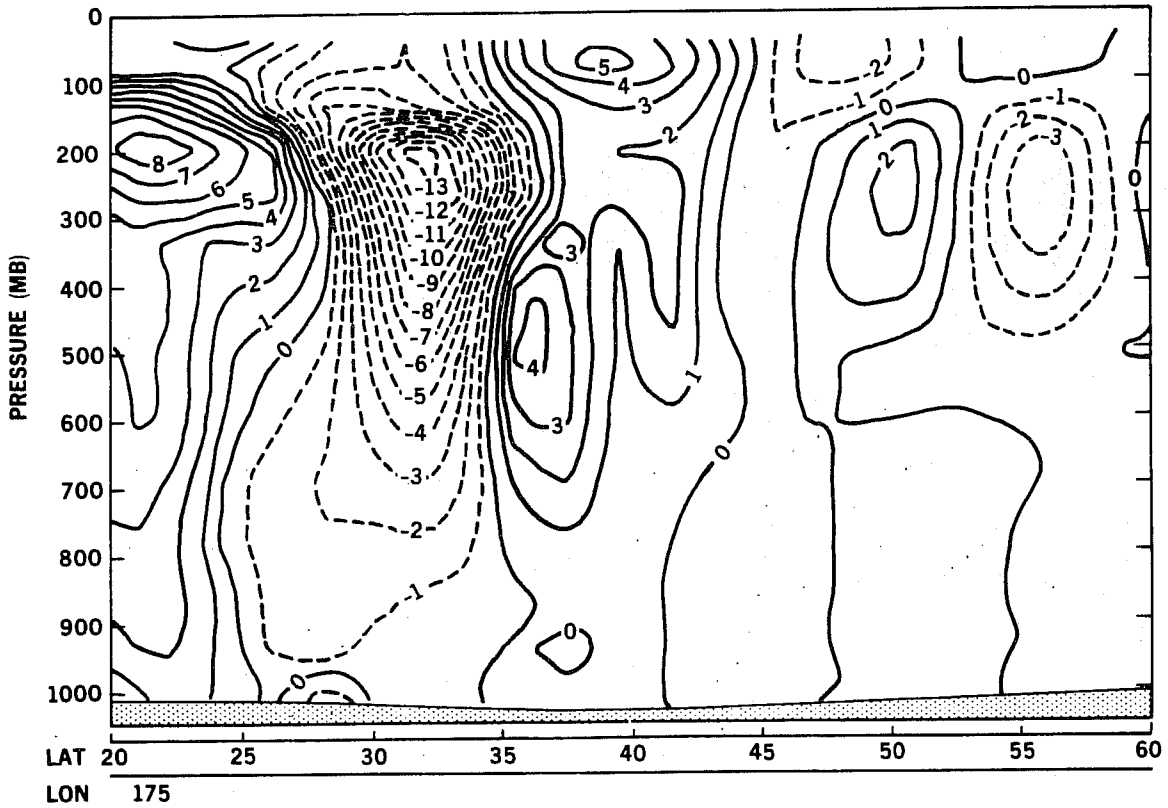


Fig. 11 Cross-section along 175°E showing differences in the westerly wind component between analyses AI and AO for 11 November.

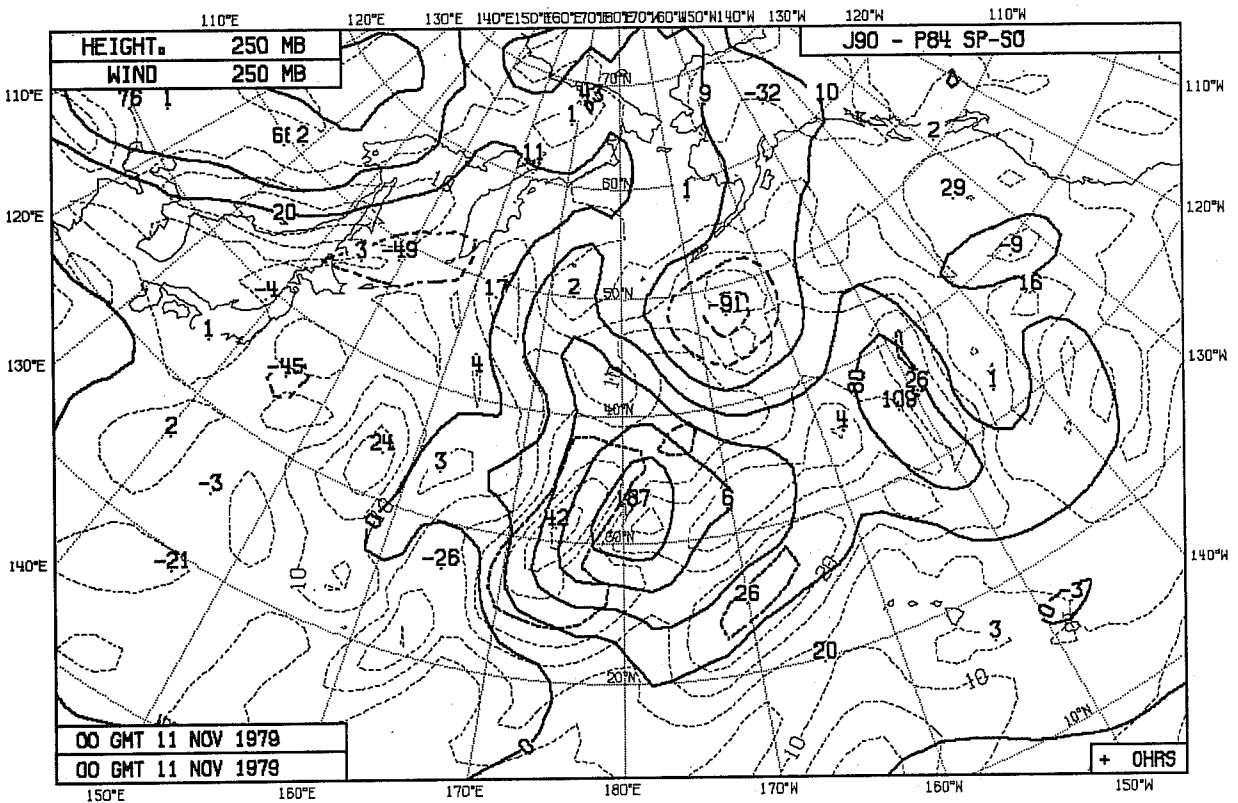


Fig. 12 As Fig. 7, but SP-SO.

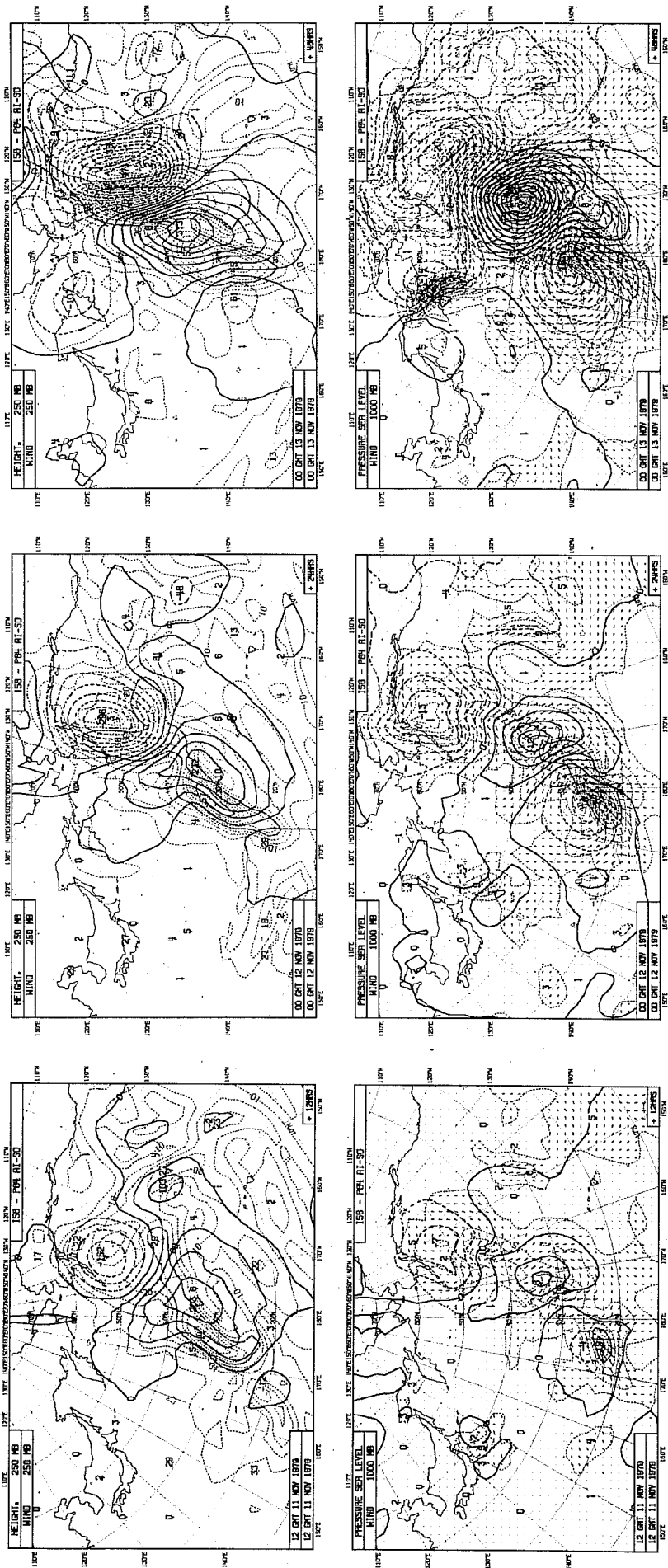


Fig. 13 Forecast difference, AI-SO, at (a) + 12h, (b) +24h and (c) +48 h.

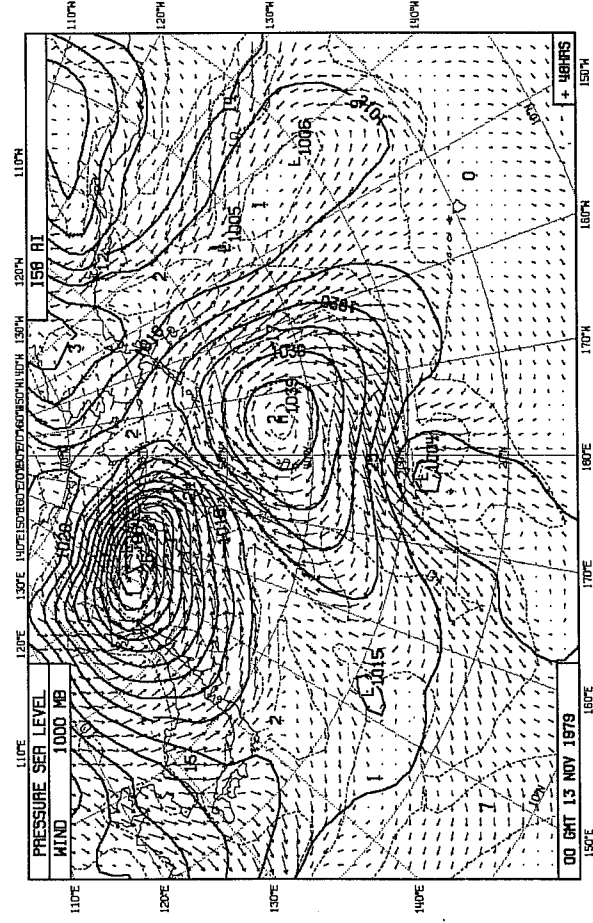
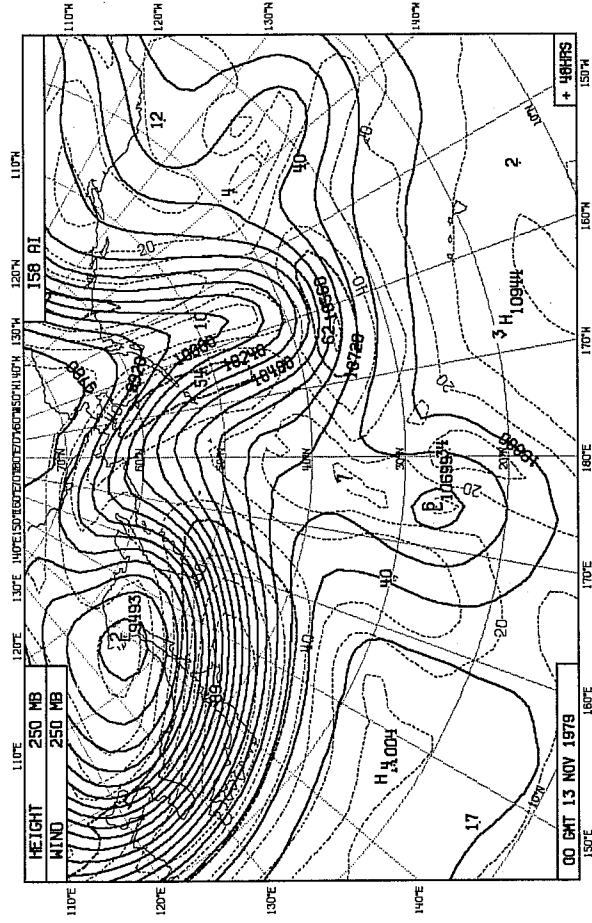


Fig. 14 48h forecasts from assimilations AI at 250mb (top) and sea level (bottom); valid 00 GMT 13 November.

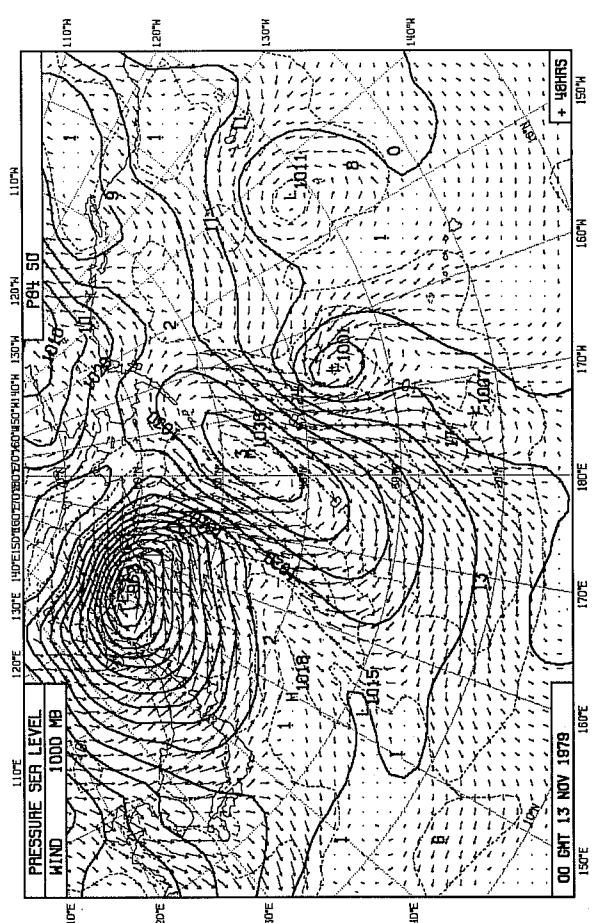
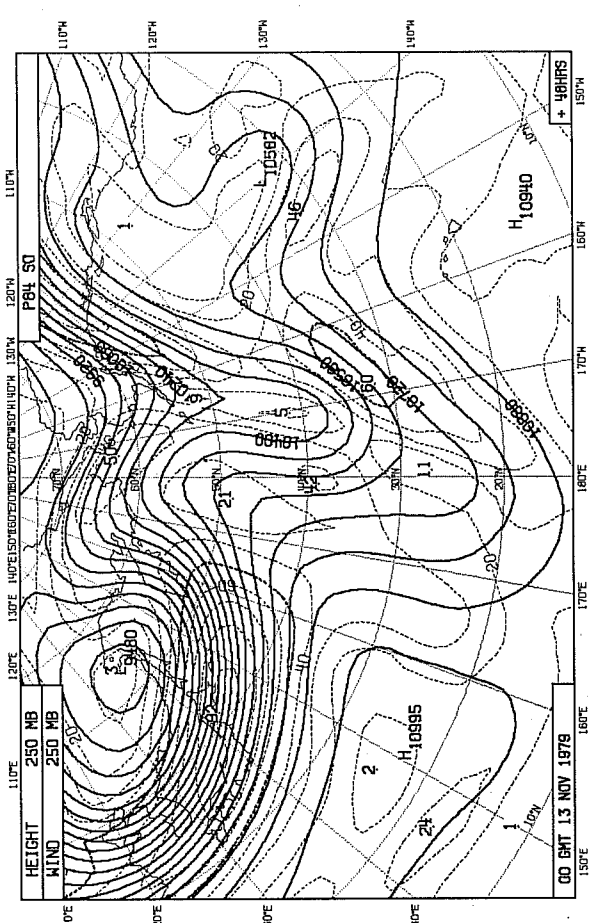


Fig. 15 As Fig. 14, but for SO.

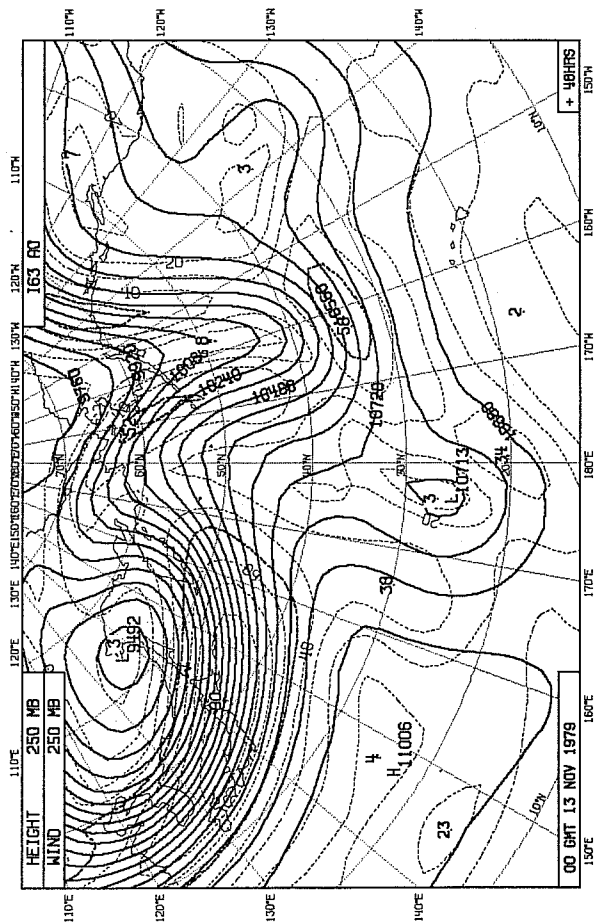


Fig. 16 As Fig. 14, but for AO.

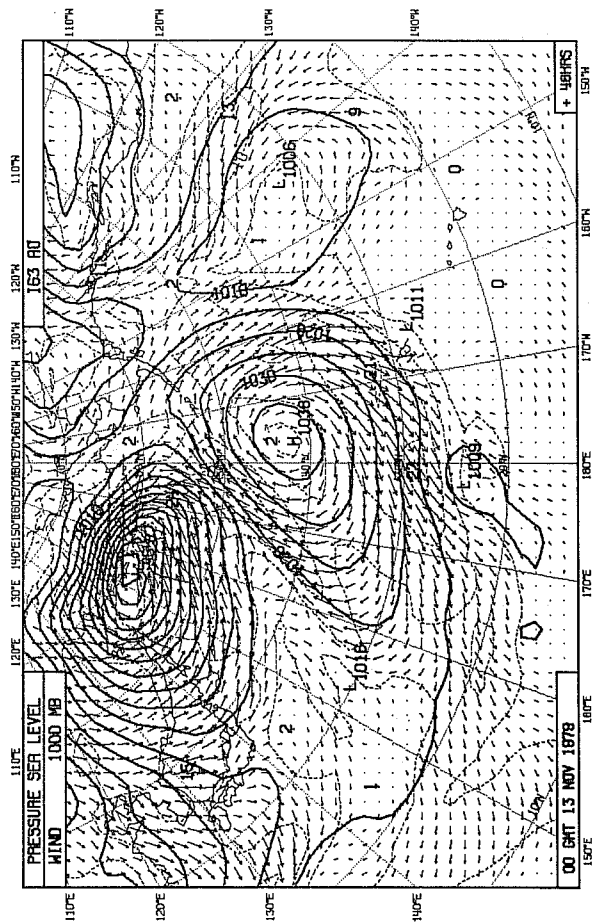
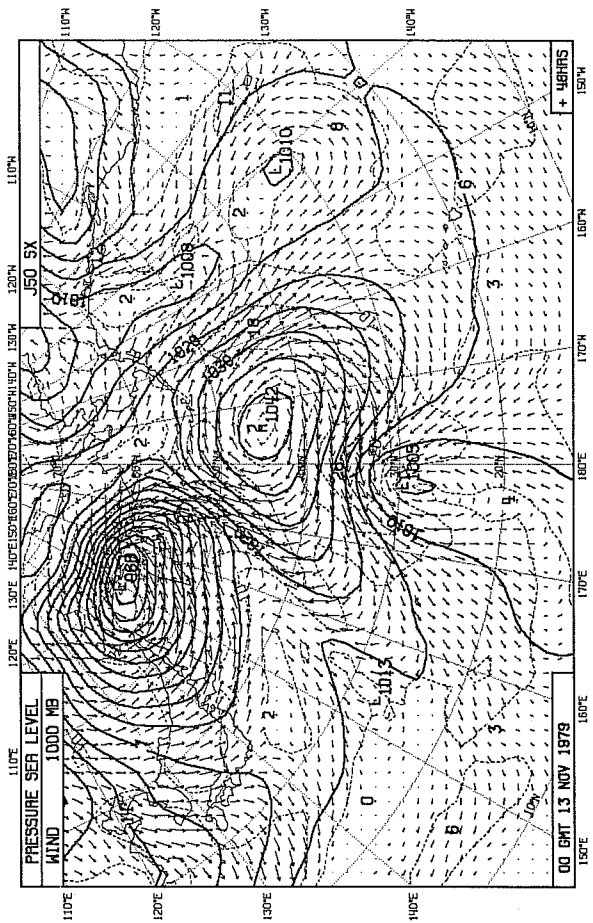
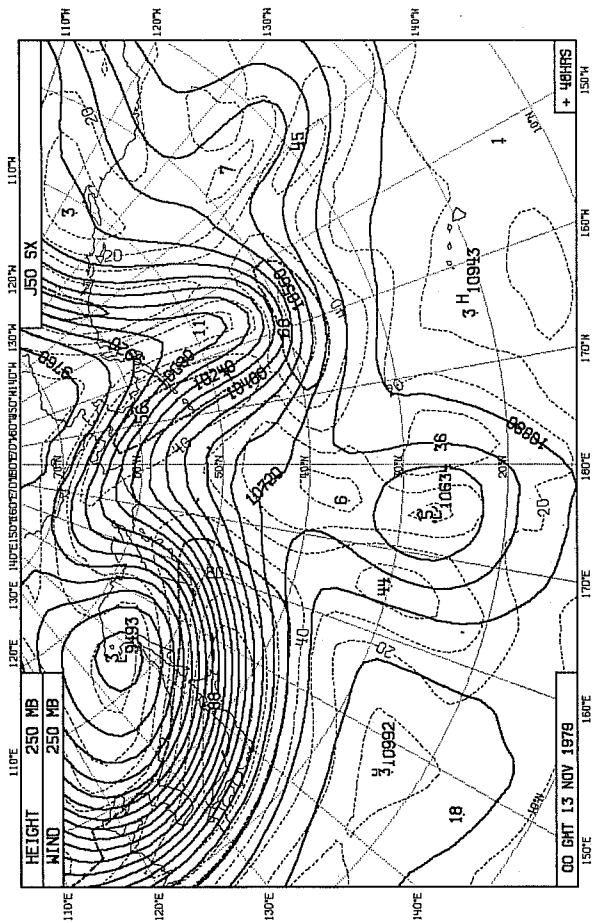


Fig. 17 As Fig. 14, but for SX.



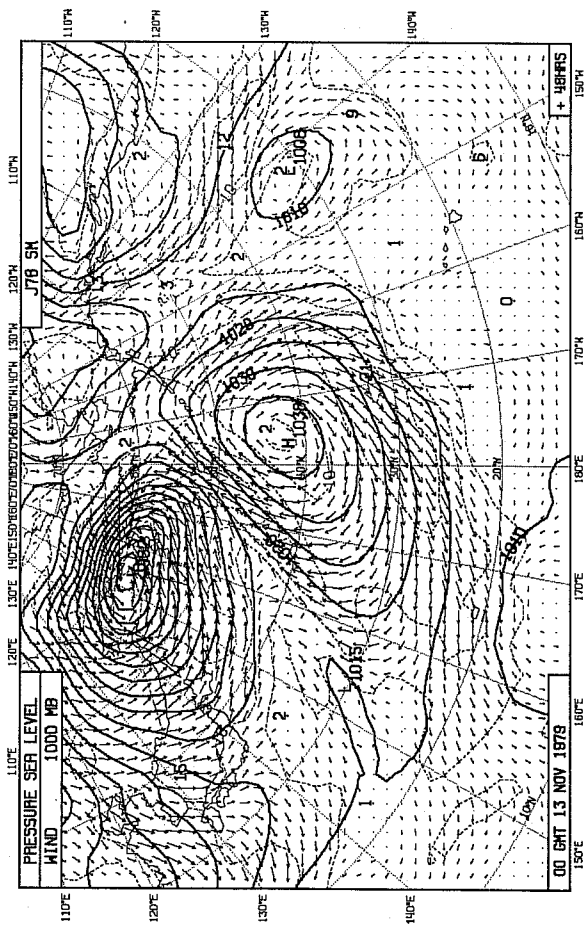
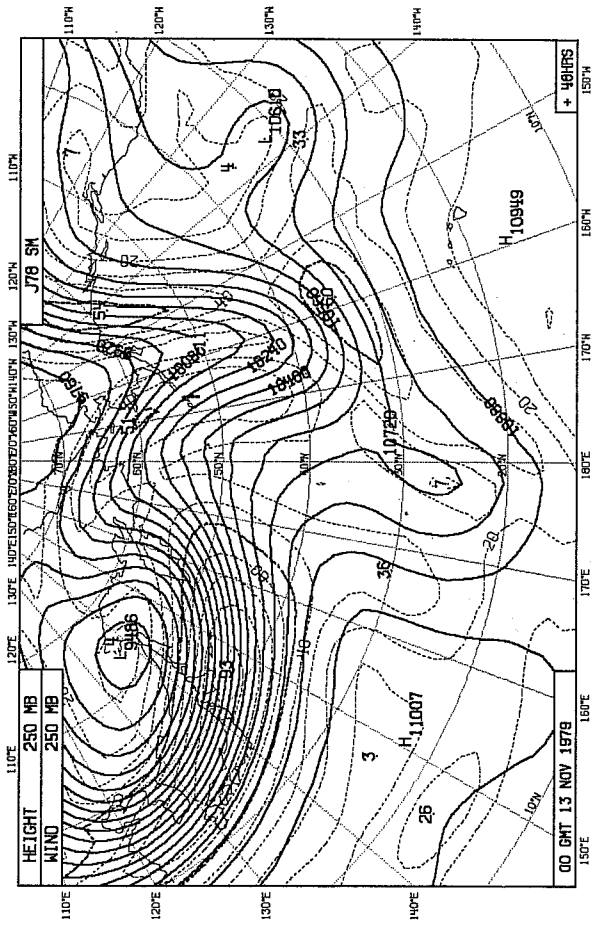
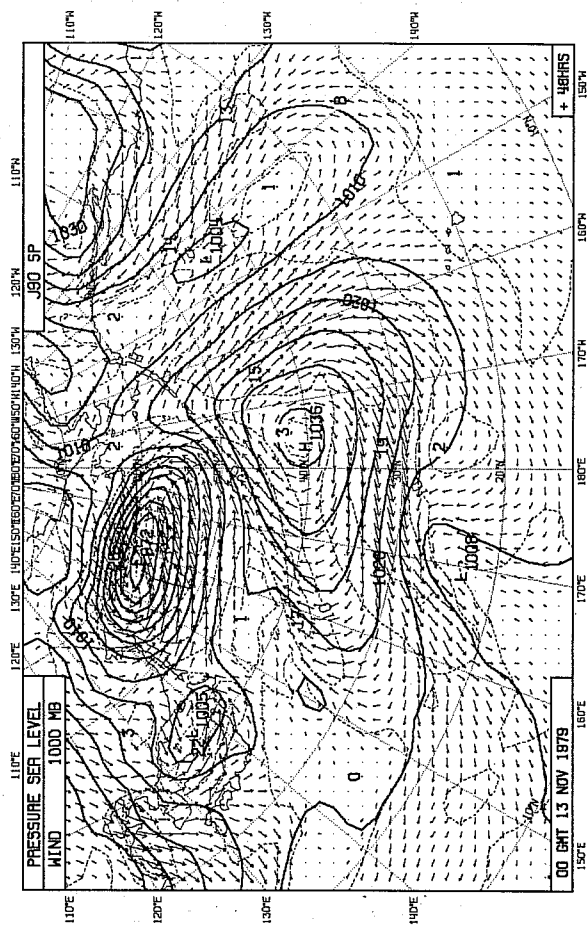
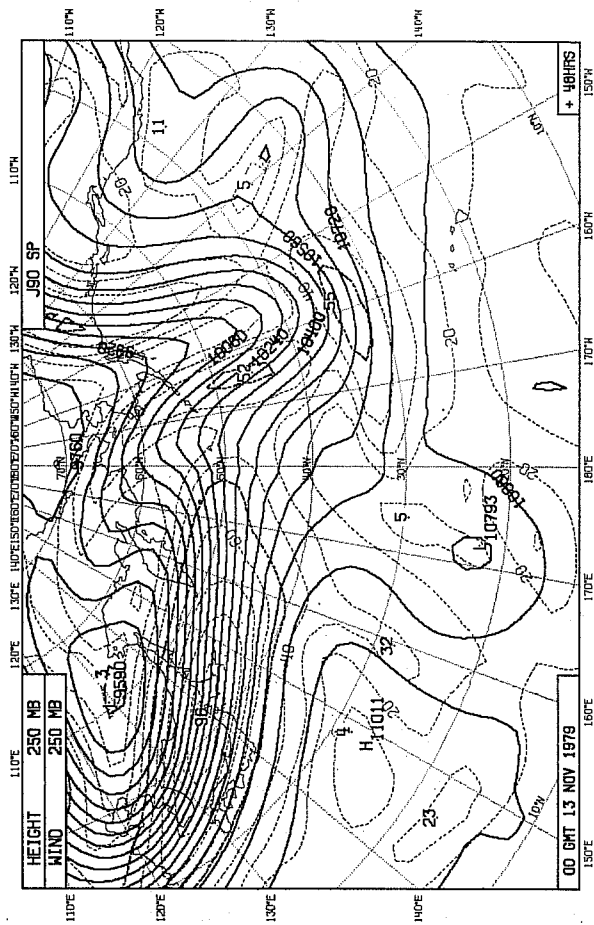


Fig. 19 As Fig. 14, but for SP.

Fig. 18 As Fig. 14, but for SM.

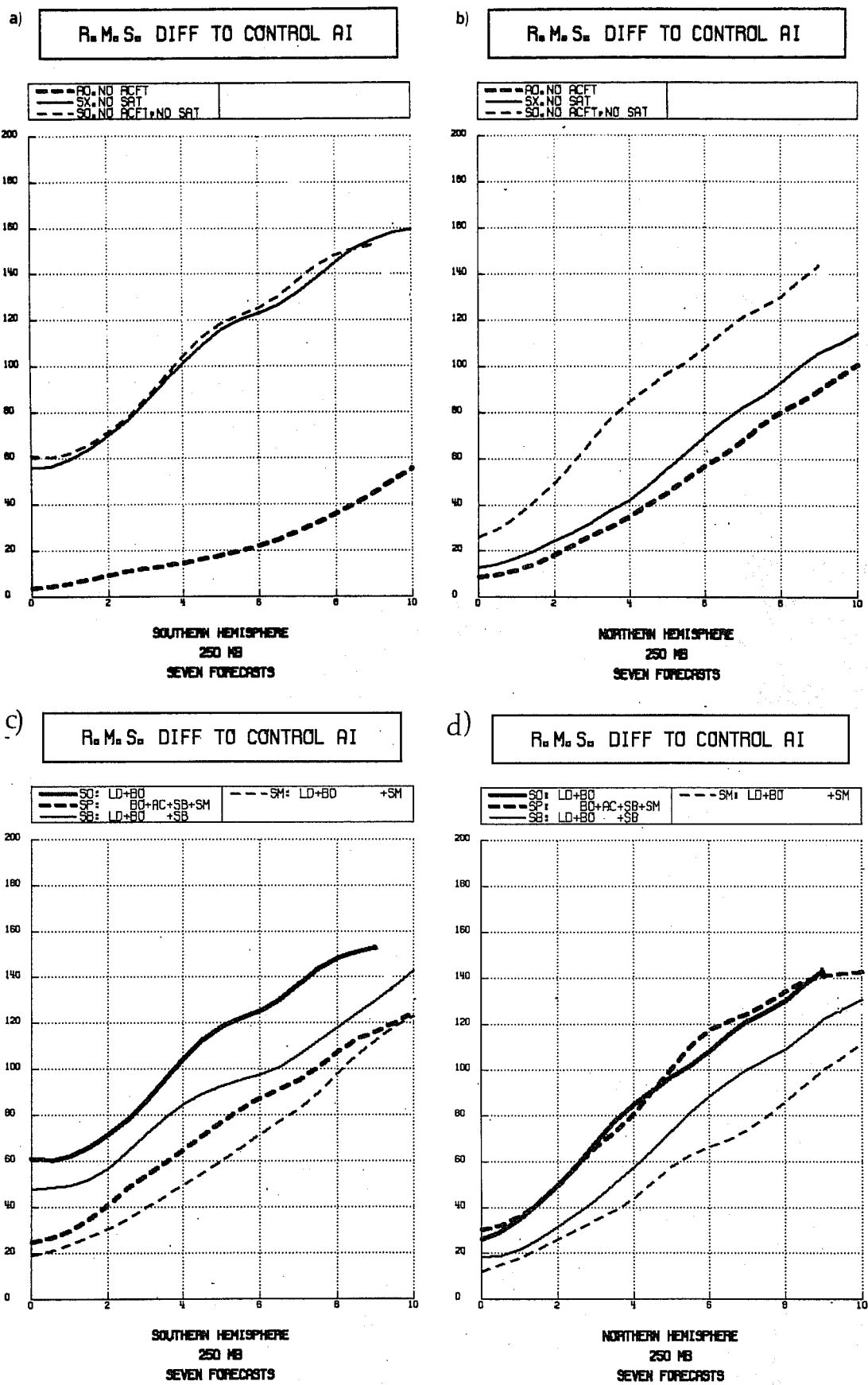


Fig. 20 Separation of forecasts between various experiments and the control assimilation AI expressed as the r.m.s. difference of the 250mb heights. Average of 7 forecasts from each assimilation experiment. See Table 1 for abbreviations.